

## *Spatial Organization of Biological Soil Crusts in Drylands*

Daniel Kozar  
Hydrologic Sciences  
djkozar@ucdavis.edu

### ***Abstract***

Given projected rises in temperature and changes in precipitation regime in many of the world's drylands, local ecosystems in water stressed regions will likely experience even greater stress in coming years. This stress can result in drastic ecosystem state change associated with die-off and nutrient losses. While researchers have paid significant attention to arid vegetation to understand risk of state change, no work has been completed on another ubiquitous dryland constituent – biological soil crusts (BSCs). BSCs live in the very top layers of the soils surface and play key roles in ecosystem processes. As BSCs are believed to respond to aridity increases before vegetation, they likely can provide a greater understanding of dryland state change. A spatially implicit population dynamics population model and a spatially explicit ecohydrological model were paired together to understand the behavior of this system and evaluate information metrics of this system in space. Population dynamics of both models generally agreed but the spatially implicit model displayed an unexpected bifurcation in BSC population. Spatial excess entropy shows that this system self-organizes when including BSCs and that self-organization is stronger at lower precipitation rates. This analysis suggests that the BSC-vegetation system is not sensitive to changes in interaction, and that BSC spatial signatures may provide information on dryland state change.

## **1. Introduction**

Ongoing climatic changes and projected increases in abiotic stress in drylands has led many researchers to ponder the fate of these already stressed landscapes. While primary productivity in drylands is low, they cover approximately 40% of the Earth's terrestrial surface, are home to 2 billion people, and play key roles in global carbon and nitrogen cycling (Belnap et al., 2016). Adaptations allow biota, mostly primary producers, to survive in drylands, but these ecosystems are highly sensitive to variation in resource availability. Non-linear responses in ecosystems to stress can cause rapid loss of biomass that likely cannot return, due to hysteresis (Scheffer, 2009). Biological soil crusts (BSCs), complex communities in the soil surface, have become a research focus in recent years and are understood to significantly affect dryland ecosystem processes. These BSCs and dryland vegetation are understood to have complex interactions. As these constituents are the primary producers in resource limited drylands, these interactions likely play a key role in community assembly and overall ecosystem stability. Despite the effort devoted to understanding regime change, these efforts focus almost exclusively on vegetation. This study provides a preliminary investigation into the role of BSCs in state change of drylands. In order to better understand BSCs, and surrounding vegetation, the system is investigated in both time and space-time. Including space into this analysis is useful as spatial metrics are often used to understand interactions of organisms and provide early warning signs for state change (Kéfi et al., 2007).

This research opens the door to a world of possibilities in understanding drylands as well provide insight into our understanding of ecosystem function. BSCs differ in composition, and therefore function, across a stress gradient, and act as natural petri dishes. Including BSCs in our models of drylands can likely help us understand anomalous behavior, better anticipate dryland response to climate change, and provide insight into solutions for dryland restoration and prevention of deterioration.

This study investigates the dynamical properties of a BSC-vegetation system in both implicit, and explicit, space. Excess entropy was also calculated in space to provide insight into self-organization and spatial complexity. Both systems exhibit similar dynamical behaviors, in accordance with qualitative expectations. Spatial excess entropy suggests that this system self-organizes and that this self-organization dissipates at higher precipitation rates. While spatial metrics are used to evaluate risk of catastrophic change in vegetation, these results suggest that BSCs may respond earlier to increases in stress, providing reason to further investigate the use of utilizing spatial metrics of these BSCs for early warning signs.

## **2. Background**

BSCs are communities of organisms living in the top millimeters to centimeters of the soils surface (Reed et al., 2019). The presence of these BSCs is facilitated by harsh dryland conditions, as less resilient competitors are absent or are only found in relatively small abundances. The primary colonizing species of BSCs are filamentous cyanobacteria, primarily of the genus *Microcoleus* (Büdel et al., 2016). These filamentous cyanobacteria secrete exopolysaccharides (EPS), which glue soil particles together and stabilize the soil surface. This increase in soil stability facilitates the immigration of higher successional BSC constituents – pigmented N-fixing cyanobacteria, lichens, and mosses, largely in that order (Read et al., 2016). Successional stage is largely limited by environmental filtering in more arid landscapes, therefore the composition of BSCs varies along an aridity gradient (Rosentreter et al., 2016). The functional role of these BSCs

also varies with respect to composition. Early successional crusts are associated with low N-fixation rates, high runoff and low biodiversity. Later successional crusts are associated with higher N-fixation, low runoff, and higher biodiversity. BSCs and vegetation are the primary biota and primary producers of drylands. Their ecological interactions are not well understood, but are thought to range from antagonistic to neutral to facilitative. Evidence suggests that BSCs and vegetation contradict the stress gradient hypothesis, which states that facilitative interactions become more abundant with higher stress. If antagonistic interactions between BSCs and vegetation do indeed increase with stress, this likely translates to abrupt loss of the inferior competitor – BSCs. In accordance with this, empirical evidence currently suggests that rises in temperature lead to significant loss in BSC cover (Johnson et al., 2012). Considering the role of BSCs in dryland processes, abrupt BSC die-off likely has drastic consequences for these ecosystems.

### 3. Dynamical System

The system in question has three states: BSCs, vegetation, and bare soil. While bare soil is not a biotic agent, it is included in this study and is seen only as a state in the spatial sense – empty parcels not occupied by BSCs or vegetation are occupied by bare soil substrate. Without the consideration of space, only two states are present: BSCs and vegetation. As no investigation has been completed yet on the modelling BSC-vegetation populations in concert, already existing models were amended to include some general understandings of the system.

#### 3.1. Spatially Implicit Model

In a finite, resource limited, ecosystem open to its surroundings, it can be assumed that a population can only grow to a maximum threshold, or carrying capacity. Therefore, the spatially implicit system included in this study is an adaptation of the logistic-growth population dynamics model including interaction terms to account for facilitation or antagonism between populations (Eqs. 1 & 2). Two states were included in this system: vegetation ( $V$ ) and BSCs ( $BSC$ ).

$$\frac{dV}{dt} = r_V V \frac{(K_V - V + \alpha_{VB} BSC)}{K_V} \quad (1)$$

$$\frac{dBSC}{dt} = r_{BSC} BSC \frac{(K_{BSC} - BSC + \frac{\alpha_{VB} V}{\beta})}{K_{BSC}} \quad (2)$$

$$\beta = \frac{\alpha_{VB}}{\alpha_{BV}} \quad (3)$$

$$\alpha_{VB} = \alpha_{VB_{max}} \frac{BSC + C + 1}{C + e^{\gamma BSC}} \quad (4)$$

Each state has an associated intrinsic growth rate ( $r_i$ ) and carrying capacity ( $K_i$ ). Interaction terms,  $\alpha_{ij}$ , correspond to the relative effect of species  $j$  on species  $i$ , and can be any real value. As mentioned previously, literature suggests that the relative strength and direction of interactions between vegetation and BSCs varies (Havrilla et al., 2019). A parameter of the quotient of each relative effect,  $\beta$ , was included to act as a proxy for variation in interaction and aridity in one parameter (Eq. 3). In accordance with findings in literature,  $\beta$  is expected to decrease and turn negative with increases in aridity. A saturation equation for the effect of BSCs on vegetation is also included such that the benefits conferred to vegetation from these BSCs decreases with BSC

population size (Eq. 4). In this equation,  $\alpha_{VB_{max}}$  is the maximum rate benefit from BSCs to vegetation,  $C$  is a population scaling rate, and  $\gamma$  is a rate of loss of vegetation benefit from BSC growth.

### 3.2. Spatially Explicit Model

The spatially explicit model used in this study is amended from an ecohydrological model (McGrath et al., 2012). The original model includes two states – vegetation and bare soil. In this study, another state was added to account for BSCs. As BSCs are photosynthetic, they can be conveniently treated similarly to vegetation in this model. Therefore, all parameters for the growth of vegetation and effects on hydraulic conductivity are included for BSCs, only their magnitudes vary.

This model uses a simple water balance to calculate the magnitudes of each component of the balance in space (Eq. 5).

$$\frac{dw_i}{dt} = P_i + R_i - Q_i - E_i - \sum_i^n T \quad (5)$$

Where  $w$  is sum of water at cell  $i$ ,  $P$  is precipitation,  $R$  is runoff,  $Q$  is groundwater flow loss,  $E$  is evaporation, and  $T$  is transpiration.  $T$  is summed not only for cell  $i$ , but all  $n$  of its immediately surrounding cells. All components of this water balance have units of mm/year. The probability of infiltration at a cell is dictated by its hydraulic conductivity ( $K_i$ ). Hydraulic conductivity is a function of the presence of both vegetation and BSCs (Eq. 6).

$$K_i = K_0 + K_v \int g_v(r) f_v(r) dr - K_{BSC} \int g_{BSC}(r) f_{BSC}(r) dr \quad (6)$$

Where  $K_0$  is the hydraulic conductivity of bare soil, and  $K_v$  and  $K_{BSC}$  are the hydraulic conductivity values for vegetation and BSCs, respectively. The functions  $g_i$  and  $f_i$  for each state correspond to the presence or absence of the state in question and an exponential decay kernel, respectively. While vegetation is accepted to increase hydraulic conductivity, BSCs are suggested to decrease hydraulic conductivity and its effect in Eq. 6 is therefore negative.

The growth and death of the biotic components in this model is only dictated by the values obtained in the water balance for a given time step. If the transpiration rate,  $T_i$ , exceeds the critical threshold for growth,  $T_v$  or  $T_{BSC}$ , the biomass of the state in the cell grows by a constant increment. If  $T_i$  for a cell with biomass is less than the relevant critical transpiration rate, the biomass decreases by the same increment. In a cell of bare soil, if the water balance at the end of a year is greater than a threshold for germination,  $wv/w_{BSC}$ , then the relevant state appears. For both the threshold transpiration and germination rates, the value corresponding to BSCs is less than the value for vegetation. It is also assumed that vegetation has a competitive advantage over BSCs, due to light interception by the canopy. Therefore, in any cell where they both are present the BSC value goes to zero. This is a rather simplified description of the ecohydrological model used in this paper so as to stay focused on the utilization of dynamical systems and information theory. For more details on the original model that the above is based on, see McGrath et al., 2012.

## 4. Methods

### 4.1. Spatially Implicit Model

Fixed point analysis of this two-dimensional system was completed by linearization of the Jacobian at each respective fixed point, as outlined in Strogatz, 2015 (Figure S1). This analysis is paired with phase portraits created using the POCI Python library. Phase portraits were run for 400 iterations over an integration time of 100. Being a natural system, neither population can be negative. Therefore, initial population values were randomly sampled between 0 and 1 for both states. Phase portrait diagrams were created along a varying interaction gradient,  $\beta$ , from -2 to 2 using parameters with reasonable values inferred from intuition based on literature (Table S1).

### 4.2. Spatially Explicit Model

The spatially explicit model was run in MATLAB using Euler's method as the time step is one year, and there is little reason in this application to reduce the time step for more accurate numerical approximation. This model was run for annual precipitation rates ranging from 200 to 400 mm year<sup>-1</sup> at 50 mm year<sup>-1</sup> increments for a time of 60 years so as to allow sufficient time for self-organization and to capture steady-state dynamics. The population of each constituent was then calculated over time to estimate dynamical behavior of each population when modelled in space. Parameters used for this model follow those included in McGrath et al., 2012, with new parameters for BSCs assumed in relation to vegetation parameters from current understanding of the system in literature (Table S2).

### 4.3. Spatial Information Metrics

Spatial excess entropy was calculated for every time step in all simulations using the methods outlined in literature (Feldman & Crutchfield, 2003)(Figure S2). High excess entropy is a measure of complexity and thus self-organization (Prokopenko et al., 2009). Excess entropy is valuable in this context because the self-organization of ecosystems is commonly linked to function. Arid vegetation often self-organizes to ameliorate the effects of stress (Deblauwe et al., 2008; Rietkerk et al., 2002). Feldman & Crutchfield, 2003 outline the calculation of excess entropy in space similarly to that of a typical temporal sequence. For a given cell in a lattice structure, the states of the "past" are sampled in order of the surrounding spatial "neighborhood" in order of closest to nearest cells to further cells in a predetermined neighborhood template (Fig. 1).

...	7	5	3	1	X				
					2	4	6	8	...

**Figure 1:** Neighborhood template around a given cell, X, in order of state-sampling to calculate spatial information metrics. Neighbors closest to X are sampled first as they are from the more recent "past"

For a given length,  $L$ , the block entropy is calculated in the same sense as Shannon entropy (Eq. 7).

$$H(L) = - \sum_{x \in X} p_i \log_2 p_i \quad (7)$$

Where  $p_i$  is the probability of a given state in the record of length  $L$ . While block entropy is calculated for binary strings using words, block entropy in this sense is calculated such that the record is for states themselves. From block entropy, the asymptotic entropy rate,  $h_\mu$ , can be calculated (Eq. 8).

$$h_\mu = \lim_{L \rightarrow \infty} \frac{H(L)}{L} \quad (8)$$

Which then allows for the calculation of excess entropy (Eq. 9):

$$E_c = \sum_{L=1}^{\infty} [h_\mu(L) - h_\mu] \quad (9)$$

This calculation can be done for every cell within a given lattice from the above synthetic data. In this study a template of  $L = 20$  was used, which well allowed for convergence to  $h_\mu$ . Therefore, from the neighborhood template, only cells at least 10 cells away from the boundary of the lattice could allow for excess entropy calculation. From these calculations the mean  $E_c$  for each lattice was calculated in time for varying precipitation depth.

## 5. Results

### 5.1. Spatially Implicit Model

Two fixed points were calculated for the spatially implicit population model included in this analysis,  $(0, 0)$  and  $(0, K_B)$ , where  $x$  and  $y$  values correspond to the populations of vegetation and BSCs, respectively. The linearized Jacobian of the system at two absent populations,  $(0,0)$ , is either an unstable node or an unstable spiral. This is assuming that the intrinsic growth rate of both populations is positive. If the intrinsic growth rate of vegetation ( $r_V$ ) exceeds that of BSCs ( $r_B$ ), the origin is an unstable node. If the intrinsic growth rate of BSCs exceeds that of vegetation, the origin is an unstable spiral. The other fixed point corresponds to a BSC population at carrying capacity with absent vegetation,  $(0, K_B)$ . This fixed point is always a saddle point as the determinant of the linearized Jacobian will always be negative. If there is no two-directional interaction between vegetation and BSCs such that the interaction parameter,  $\beta$ , is zero, a stable node will occur at the respective carrying capacities of each population –  $(K_V, K_{BSC})$ .

Phase portraits created for this two-dimensional system agree with predicted behaviors from the fixed-point analysis described above (Fig. 2a-c). Assuming positive initial values and small maximum effect from BSC-vegetation,  $\alpha_{VB}$ , relative to intrinsic growth rates, phase portrait trajectories for varying  $\beta$  show that populations grow and flow away from the origin to values corresponding to each carrying capacity (Fig. 2a-c). If the magnitude of  $\alpha_{VB}$  greatly increases and is equal to, or greater than, the magnitude of the intrinsic growth rates, it allows for the populations to grow far beyond their carrying capacities (Fig. 2d). This behavior is, however, unlikely in natural systems as relatively low  $\alpha_{VB}$  limits the continuous growth of both populations. These results suggest that these populations are rather stable to changes in interaction strength and that variation in stress has little effect on either population if modelled as a two-state system.

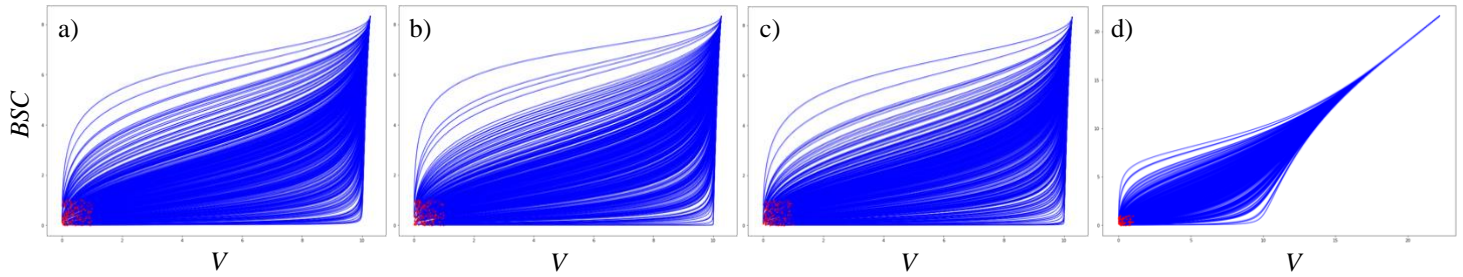


**Figure 2:** Phase portrait diagrams for the spatially implicit system at a constant  $\alpha_{VB_{max}} = 0.05$  for (a)  $\beta = -1$ , (b)  $\beta = 0$ , and (c)  $\beta = 1$ . At  $\beta = 1$  and  $\alpha_{VB_{max}} = 0.05$ , (d) shows that this facilitative interaction can cause populations to far exceed their carrying capacities

### 5.2. Spatially Explicit Model

Simulations of vegetation and BSCs in space and time yield generally similar behaviors to those in time only and spatial patterns agree with those observed in these ecosystems. Information metrics also demonstrate that the system exhibits higher levels of self-organization at low precipitation values.

Before discussing population dynamics or information metrics in space, it is worth noting the spatial patterning of the synthetic data used in this study. The original unamended model recreates vegetation bands on dryland hillslopes and only models vegetation biomass. By adding another state to this model, the behavior in space could be very different from the original. Simply from visual inspection one can see that these vegetation “tiger bush” patterns still emerge (Fig. 3). BSCs are seen in the interspaces between vegetation bands, which agrees with field observations (Eldridge et al., 2000). Cyanobacterial crusts, which reduce hydraulic conductivity and promote runoff, are considered to be critical in allocating water to downslope vegetation. As this is the first time a spatially explicit model including vegetation and BSCs has been created, this is rather promising.

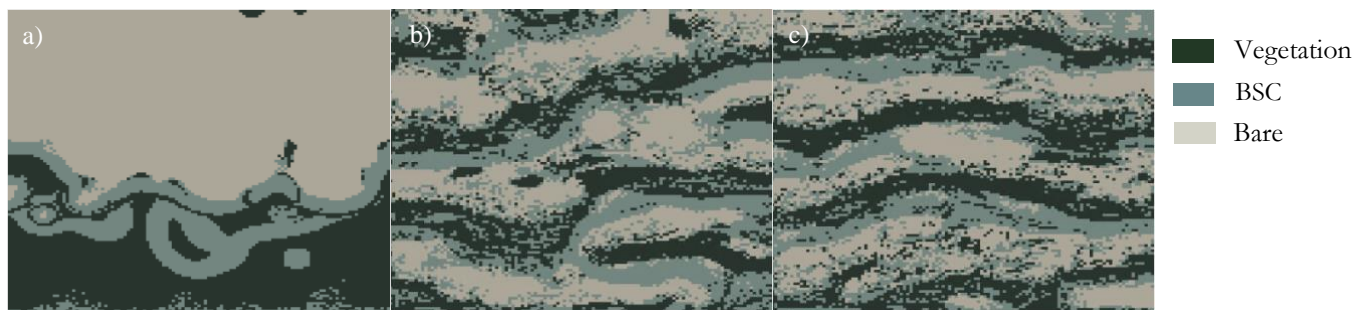


**Figure 3:** Modelled states in space for (a)  $P = 200 \text{ mm year}^{-1}$ , (b)  $P = 300 \text{ mm year}^{-1}$ , and (c)  $P = 400 \text{ mm year}^{-1}$  in the spatially explicit model

Population dynamics of each constituent in space generally show convergence on a stable population for both constituents (Fig. 4). The population size of each component is not so important here so much as the dynamical behavior, so only behavior is considered. For all precipitation rates, vegetation converges on a population of approximately 4200 cells. For precipitation rates 300-400  $\text{mm year}^{-1}$ , BSCs reached a stable population of approximately 5500 cells. For precipitation values less than 300  $\text{mm year}^{-1}$ , BSCs oscillate at much lower

populations. The vegetation populations for these low precipitation rates oscillate as well but around the stable population of vegetation in all other simulations. This may have a simple explanation. If resource (water) allocation is very low, the superior competitor (vegetation) will cluster together due to an island of high hydraulic conductivity. BSCs establish on the upper edges of the vegetation patch (Fig. 3a) from small storage surplus in the water balance. As these BSCs provide water to downslope vegetation, the adjacent vegetation cells grow and then outcompete these BSCs. The process then repeats. This oscillatory behavior is not expected from analysis of the spatially implicit population model, highlighting the need for further investigation.

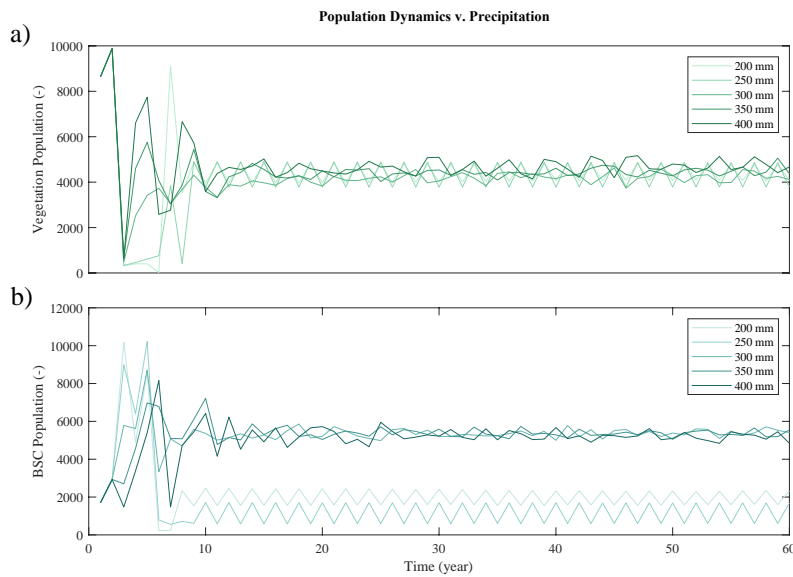


**Figure 4:** Populations, or cell count, in the spatially explicit model along an aridity gradient for the two biotic states (a) vegetation, and (b) BSCs

Spatial excess entropy,  $E_c$ , in time suggests that the system self-organizes when precipitation is above a threshold of  $300 \text{ mm year}^{-1}$  and that lower precipitation rates above this threshold exhibit greater self-organization than higher precipitation rates (Fig.5).  $E_c$  for precipitation rates above this threshold show a spike in time steps 0-20, which then decreases. This corresponds to an initial period of self-organization, which induces an increase in complexity, captured by  $E_c$ . After this initial period of self-organization, however,  $E_c$  decreases. This rate of decrease is suggested to negatively correlate with stress, as higher precipitation exhibits greater loss of complexity. As water stress induces self-organized patterns in dryland vegetation, these findings align with literature. Average spatial  $E_c$  oscillates at low values for precipitation rates less than the aforementioned critical threshold of  $300 \text{ mm year}^{-1}$ . This may be explained by zero  $E_c$  in cells where their neighborhood is homogeneous and fully predictable – there is no apparent randomness to be “explained away”.

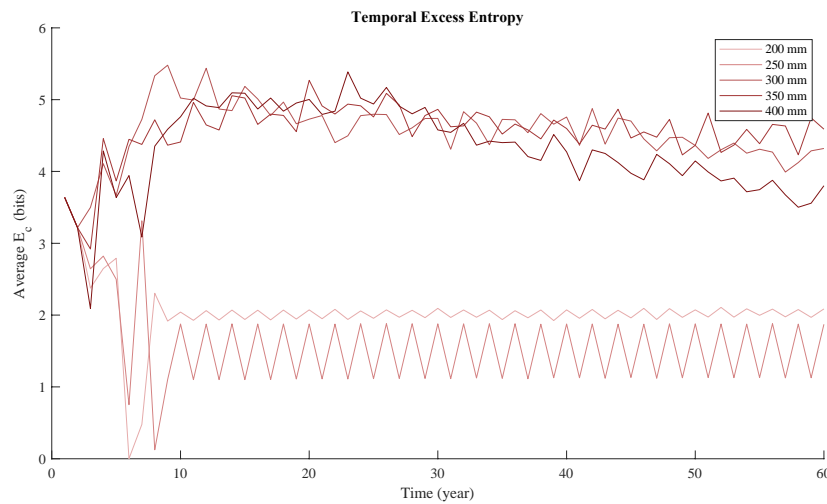


**Figure 5:** Spatially averaged excess entropy,  $E_c$ , in space along an aridity gradient. An early spike in  $E_c$  suggests self-organization, which dissipates faster at high precipitation. Low annual precipitation shows low magnitude oscillating  $E_c$  values

## 6. Conclusion

Pairing a spatially explicit model with a simple two-state logistic growth model for BSCs and vegetation yields results that agree with observed behaviors of these systems. Modelled patterns in space when adding a BSC state did not stray from real-world observations, which in itself is auspicious. While spatial patterns were not analyzed in this study due to time constraints, increased excess entropy at precipitation rates near a critical threshold suggests that there may be a BSC spatial signature that can be used as an early warning sign of state change. Despite modelled changes in aridity, this systems behavior was unaffected when modelled only in time. Population dynamics of the system modelled in space largely agree with time-only simulations, but show a bifurcation in BSC population behavior when precipitation dropped below a critical value. There is clearly much more work to be done, but these results provide a significant step forward in understanding the role of BSCs in the fate of drylands.

## References

- Belnap, J., Weber, B., & Büdel, B. (2016). Biological Soil Crusts as an Organizing Principle in Drylands. In B. Weber, B. Büdel, & J. Belnap (Eds.), *Biological Soil Crusts: An Organizing Principle in Drylands* (pp. 3–13). Cham: Springer International Publishing. [https://doi.org/10.1007/978-3-319-30214-0\\_1](https://doi.org/10.1007/978-3-319-30214-0_1)
- Büdel, B., Dulić, T., Darienko, T., Rybalka, N., & Friedl, T. (2016). Cyanobacteria and Algae of Biological Soil Crusts. In *Biological Soil Crusts: An Organizing Principle in Drylands* (pp. 55–80). Ecological Studies (Analysis and Synthesis), vol 226. [https://doi.org/10.1007/978-3-319-30214-0\\_4](https://doi.org/10.1007/978-3-319-30214-0_4)
- Deblauwe, V., Barbier, N., Couteron, P., Lejeune, O., & Bogaert, J. (2008). The global biogeography of semi-arid periodic vegetation patterns, 715–723. <https://doi.org/10.1111/j.1466-8238.2008.00413.x>
- Eldridge, D. J., Zaady, E., & Shachak, M. (2000). Infiltration through three contrasting biological soil crusts in patterned landscapes in the Negev, Israel. *Catena*, 40(3), 323–336. [https://doi.org/10.1016/S0341-8162\(00\)00082-5](https://doi.org/10.1016/S0341-8162(00)00082-5)

- Feldman, D. P., & Crutchfield, J. P. (2003). Structural information in two-dimensional patterns: Entropy convergence and excess entropy. *Physical Review E - Statistical Physics, Plasmas, Fluids, and Related Interdisciplinary Topics*, *67*(5), 9. <https://doi.org/10.1103/PhysRevE.67.051104>
- Havrilla, C. A., Chaudhary, V. B., Ferrenberg, S., Antoninka, A. J., Belnap, J., Bowker, M. A., et al. (2019). Towards a predictive framework for biocrust mediation of plant performance: A meta-analysis. *Journal of Ecology*, *107*(6), 2789–2807. <https://doi.org/10.1111/1365-2745.13269>
- Johnson, S. L., Kuske, C. R., Carney, T. D., Housman, D. C., Gallegos-Graves, L. V., & Belnap, J. (2012). Increased temperature and altered summer precipitation have differential effects on biological soil crusts in a dryland ecosystem. *Global Change Biology*, *18*(8), 2583–2593. <https://doi.org/10.1111/j.1365-2486.2012.02709.x>
- Kéfi, S., Rietkerk, M., van Baalen, M., & Loreau, M. (2007). Local facilitation, bistability and transitions in arid ecosystems. *Theoretical Population Biology*, *71*(3), 367–379. <https://doi.org/10.1016/j.tpb.2006.09.003>
- Mcgrath, G. S., Paik, K., & Hinz, C. (2012). Microtopography alters self-organized vegetation patterns in water-limited ecosystems, *117*(September 2011), 1–19. <https://doi.org/10.1029/2011JG001870>
- Prokopenko, M., Boschetti, F., & Ryan, A. J. (2009). An information-theoretic primer on complexity, self-organization, and emergence. *Complexity*, *15*(1), 11–28. <https://doi.org/10.1002/cplx.20249>
- Read, C. F., Elith, J., & Vesk, P. A. (2016). Testing a model of biological soil crust succession. *Journal of Vegetation Science*, *27*(1), 176–186. <https://doi.org/10.1111/jvs.12332>
- Reed, S. C., Delgado-Baquerizo, M., & Ferrenberg, S. (2019). Biocrust science and global change. *New Phytologist*, *223*(3), 1047–1051. <https://doi.org/10.1111/nph.15992>
- Rietkerk, M., Boerlijst, M. C., Van Langevelde, F., HilleRisLambers, R., Van de Koppel, J., Kumar, L., et al. (2002). Self-organization of vegetation in arid ecosystems. *American Naturalist*, *160*(4), 524–530. <https://doi.org/10.1086/342078>
- Rosentreter, R., Eldridge, D. J., Westberg, M., Williams, L., & Grube, M. (2016). Structure, Composition, and Function of Biocrust Lichen Communities. In *Biological Soil Crusts: An Organizing Principle in Drylands* (pp. 121–138). Ecological Studies (Analysis and Synthesis), vol 226. [https://doi.org/10.1007/978-3-319-30214-0\\_7](https://doi.org/10.1007/978-3-319-30214-0_7)
- Scheffer, M. (2009). *Critical Transitions in Nature and Society*. Princeton University Press. <https://doi.org/10.2307/j.ctv173f1g1>

## Supplementary Materials

$$\begin{aligned}\frac{\partial f}{\partial V} &= r_V - 2\frac{r_V}{k_V}V + \frac{r_C\alpha_{VB}}{K_V}B & \frac{\partial g}{\partial V} &= \frac{r_B\alpha_{VB}}{K_B\beta}B \\ \frac{\partial f}{\partial B} &= \frac{r_C\alpha_{VB}}{K_V}V & \frac{\partial g}{\partial B} &= r_B - 2\frac{r_B}{k_B}B + \frac{r_C\alpha_{VB}}{K_B\beta}V\end{aligned}$$

**Figure S1:** Equations for elements of Jacobian of two-dimensional spatially implicit system included in this study where the rate of change of vegetation corresponds to  $f$ , and the rate of change of BSCs corresponds to  $g$ .

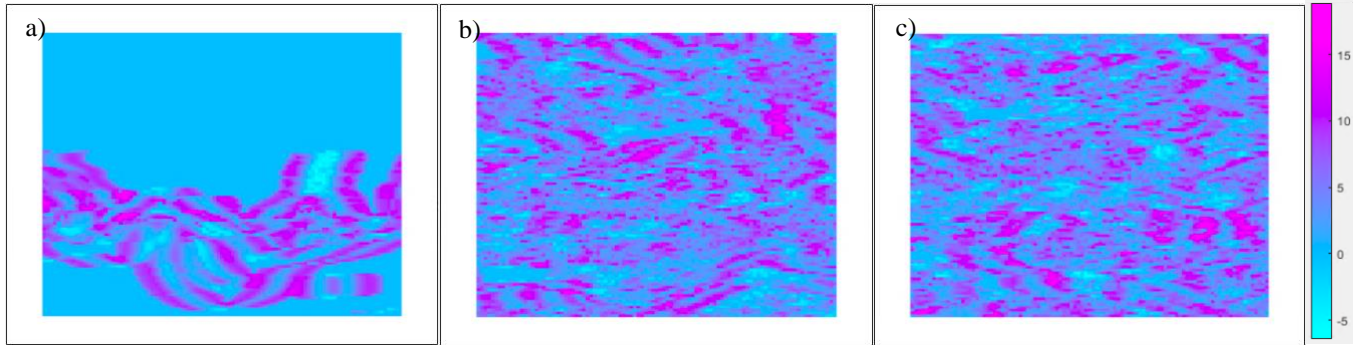


**Figure S2:** Modelled  $E_c$  in space for (a)  $P = 200 \text{ mm year}^{-1}$ , (b)  $P = 300 \text{ mm year}^{-1}$ , and (c)  $P = 400 \text{ mm year}^{-1}$  in the spatially explicit model.

Parameter	Practical Interpretation	Value
$r_V$	Vegetation intrinsic growth rate	0.2
$r_{BSC}$	BSC intrinsic growth rate	0.1
$K_V$	Vegetation carrying capacity	10
$K_{BSC}$	BSC carrying capacity	8
$\alpha_{VB_{max}}$	Maximum vegetation benefit rate	0.05
$C$	Population scaling factor	100
$\gamma$	Benefit loss rate	0.1

**Table S1:** Parameter values of the spatially implicit model

Parameter	Practical Interpretation	Value
$k_{BSC}$	BSC facilitation parameter	$0.8k_V$
$K_{BSC}$	BSC hydraulic conductivity	$0.33K_{BSC}$
$E_{BSC}$	BSC evaporation coefficient	$1.2E_V$
$T_{c,BSC}$	Transpiration threshold for BSC growth	$0.5T_V$
$w_{c,BSC}$	Water balance threshold for BSC germination	$0.5w_V$

**Table S2:** Values for new BSC parameters in spatially explicit model